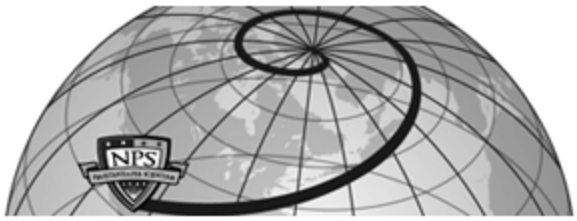

DIRECT DECAY HALF-LIFE MEASUREMENTS OF ISOMERIC STATES OF HF^{178}, HF^{179}, AND YB^{177}

JOHN C. GRIGGS
and
ALEXANDER R. MACDONALD

DIRECT DECAY HALF-LIFE MEASUREMENTS OF ISOMERIC STATES OF HF^{178}, HF^{179}, AND YB^{177}

* * * * *

John C. Griggs

and

Alexander R. Macdonald

DIRECT DECAY HALF-LIFE MEASUREMENTS OF ISOMERIC STATES OF HF^{178}, HF^{179}, AND YB^{177}

by

John C. Griggs

Captain, United States Army

and

Alexander R. Macdonald

Captain, United States Army

Submitted in partial fulfillment of
the requirements for the degree of

MASTER OF SCIENCE
IN
PHYSICS

United States Naval Postgraduate School
Monterey, California

1 9 6 3

DIRECT DECAY HALF-LIFE MEASUREMENTS OF ISOMERIC STATES OF HF^{178}, HF^{179}, AND YB^{177}

by

John C. Griggs

and

Alexander R. Macdonald

This work is accepted as fulfilling
the thesis requirements for the degree of
MASTER OF SCIENCE
IN
PHYSICS
from the
United States Naval Postgraduate School

ABSTRACT

Half-lives of thermal neutron activated samples were determined by direct decay measurements. Transport of samples between activation and counting areas was accomplished by employment of a rapid pneumatic transfer system. Use of a single channel analyser with a fast chart recorder to record scaled counts vs. time, and analysis of these data in a computer program are discussed. Results for nuclides investigated:

Hf^{178m} $t_{\frac{1}{2}} = (3.92 \pm .05)$ sec.

Hf^{179m} $t_{\frac{1}{2}} = (18.49 \pm .04)$ sec.

Yb^{177m} $t_{\frac{1}{2}} = (6.49 \pm .03)$ sec.

Our method has several advantages over multichannel devices and appears to be capable of measuring half-lives on the order of .5 seconds with approximately 1% precision.

The authors appreciate the assistance rendered by the following professors in various phases of the program: E. A. Milne and W. W. Hawes, for supervising reactor operations whenever called; J. R. Borstings, for advice on statistical matters; and H. E. Handler, for general counseling and assistance throughout the program. The authors also wish to acknowledge the assistance Prof. G. W. Rodeback, thesis advisor, gave during this project.

TABLE OF CONTENTS

LIST OF ILLUSTRATIONS

I. Introduction

Comprehensive investigations of isomeric states of isotopes of Hafnium and Ytterbium have been reported several times since the discovery of nuclear isomers /1-5/. The results of the half-life measurements reported by E. C. Campbell and P. F. Fettweis in 1959 /4/ are summarized in the following table, along with the corresponding reactions used and the gamma energies detected.

reaction	half-life	gamma energy
Yb^{176} (n,γ) Yb^{177m}	$T_{\frac{1}{2}} = 6.5$ sec	.10 Mev
Hf^{177} (n,γ) Hf^{178m}	$T_{\frac{1}{2}} = 3.5$ sec	.33, .44 Mev
Ta^{178} k capture Hf^{178m}	$T_{\frac{1}{2}} = 4.8$ sec	.8 Mev
Hf^{178} (n,γ) Hf^{179m}	$T_{\frac{1}{2}} = 18.6$ sec	.22 Mev

Of interest is the apparent difference in their results for the half-life of Hf^{178m}, although this may have been within the limits of the experimental errors, which were not reported. More recent work (1962) by K. F. Alexander and H. F. Brinckmann /5/ indicates half-lives of (4.3 ± 0.1) sec and (18.6 ± 0.8) sec for the $Hf^{177,178}$ (n,γ) $Hf^{178m,179m}$ reactions.

The objective of this work has been to improve the precision of the half-life measurements of Yb^{177m}, Hf^{178m}, and Hf^{179m}. Measurements were made by scintillation crystal detection of direct gamma decay of thermal neutron activated samples. The time delay between activation and measurement was minimized through the use of a rapid pneumatic transfer system which transfers the sample from the activation region to the counting area. Use of a single channel analyser and fast scaler kept

dead times below those commonly encountered with multichannel instruments. A fast continuous-chart recorder was employed for accurate recording of data.

Data was analysed in a computer program (FRANTIC II, by P. C. Rogers of M.I.T.) /6/ which performs an iterative least squares analysis of multiple exponential decays. Several runs have been made for each nuclide, not only to check reproducibility of the measurements, but also to determine mean half-life values based on statistical weighting and the corresponding error estimates for these mean half-lives.

II. Experimental Equipment (Schematic, Fig. 1)

A. Transfer System

1. The rapid pneumatic transfer system was designed and built for use in the AGN-201* reactor at USNPGS by Paas and Sullivan /7/. It transports a sample, which is placed in a small light container, from the counting area, about eight feet from the reactor shielding, into a high neutron flux region in the reactor core. Here the sample is activated by slow neutrons and then propelled under positive pressure back into the counting position. Transit time from core to counting position is approximately one-tenth second. The transfer system is completely closed, allowing recycling of the sample without disturbing the detection arrangement.

2. The sample container, or "rabbit", is made of balsa wood in the shape of a bullet. It is 4.5 cm long, has a 1.9 cm diameter, and weighs about 1.1 g including the sample. The isotopically enriched sample, 50 mg in powdered form, was placed in a gelatin medicinal capsule which was then secured within the "rabbit". Irradiation and counting of a dummy "rabbit" (less sample) indicated no increase over background rates.

*The AGN-201 is a graphite and polyethylene-moderated research reactor capable of producing a neutron flux up to 4 x 10^{10} n/cm^2sec at the AEC license limit of 1000 watts.

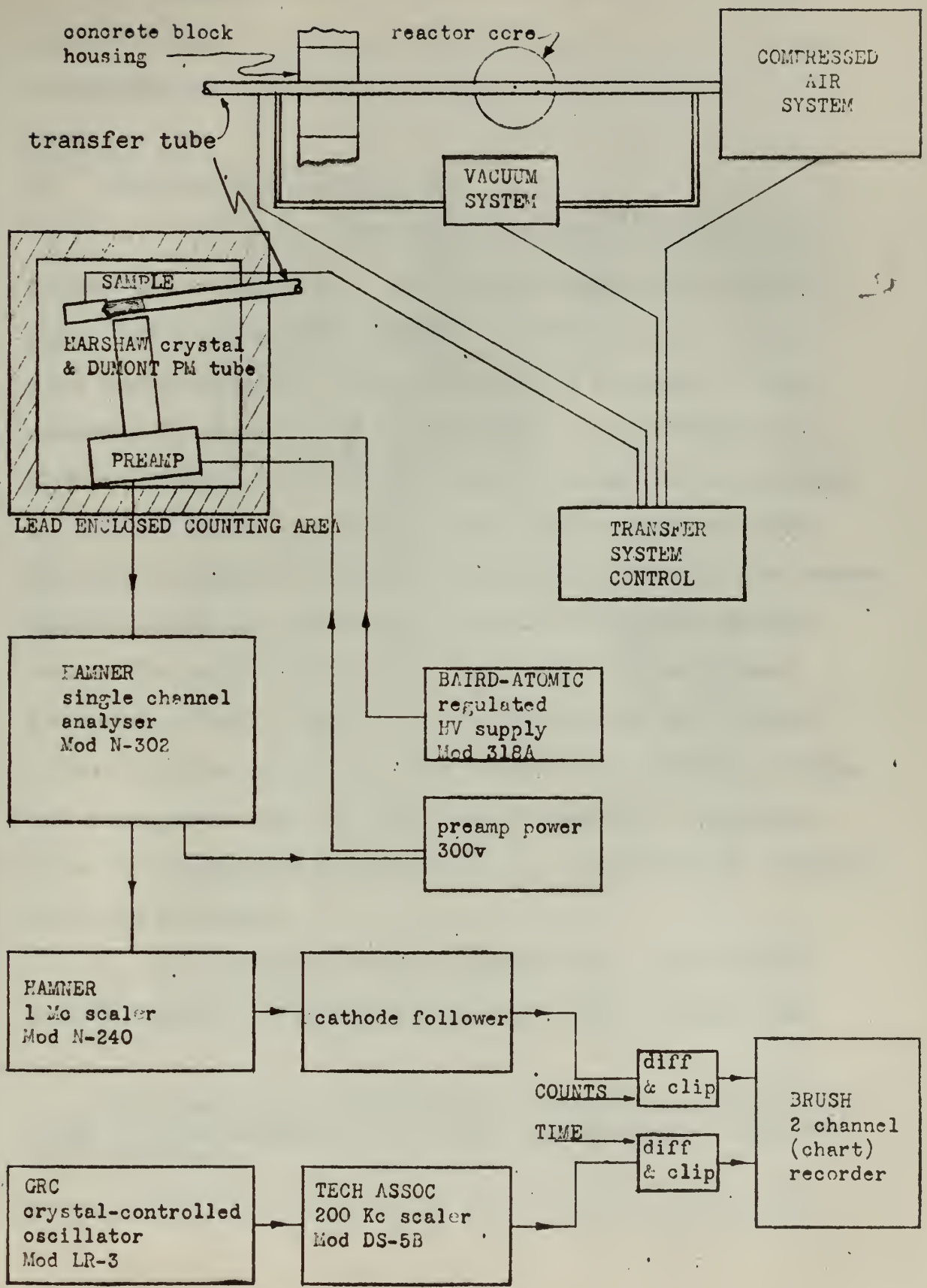

Figure 1.

Counting System and Pneumatic Transfer System

3. Samples were procured from Oak Ridge National Laboratory and are highly enriched in the nuclides under investigation. Isotopic analyses are included as Appendix III.

B. Detector System (Fig. 2)

1. A 2" x 2" NaI(Tl) crystal was used as the scintillation detector. The crystal used was a Harshaw Model 8S8/2-I integral assembly incorporating a Dumont 6292 photomultiplier tube with an S-11 response. The assembly is rated by the manufacturer to be capable of 7.6% resolution.* Our measurements showed the resolution to be 8.0% at the recommended 1000 volts anode-cathode operating voltage. During counting, the crystal was seated flush against the rabbit tube in the shielded counting area. The shielding material was lead with a minimum thickness of two inches. The counting area was off-set about 16 inches from the rabbit tube center-line to reduce the background rate at high reactor powers. A typical value of background is one count per second at an operating power of 20 watts.

2. The crystal-PM tube assembly was connected to a 6AK5 cathode-follower preamplifier which relayed the

*The resolution is defined as the ratio of the energy width at half maximum to the mean energy of the .662 Mev Cs^{137} photopeak.

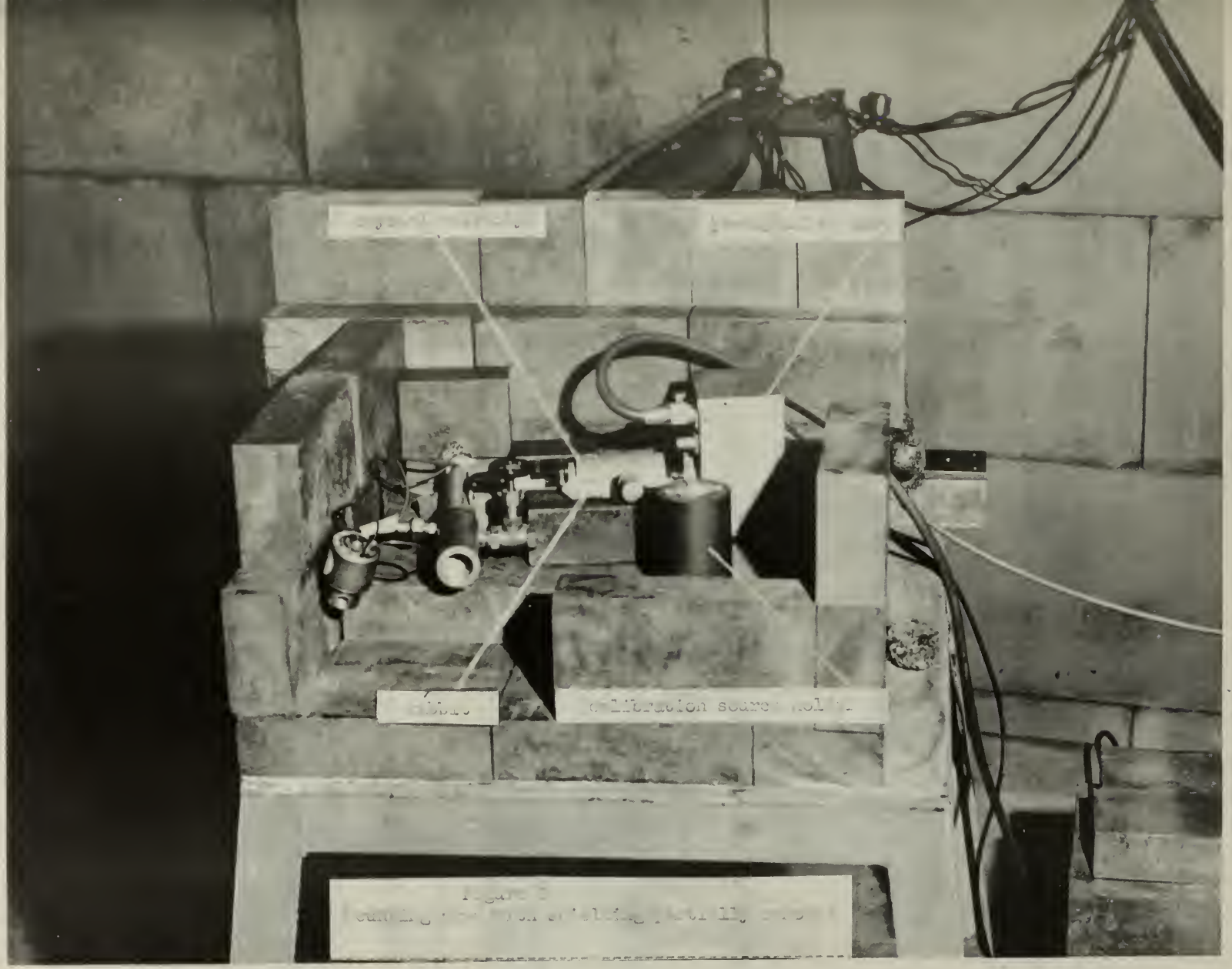

signal through 50 feet of shielded cable to the input of the linear amplifier.

3. High voltage for the photomultiplier tube was furnished by a regulated power supply with a specified stability of less than .0026% output change per line volt input change, and a maximum output change of .2% per day. No significant H. V. drift was observed during the decay runs. Preamplifier power (+300v.) was supplied by a stabilized power supply unit in the single channel analyser.

C. Single Channel Analyser

A commercial combination nonoverload linear amplifier and integral-differential discriminator was used. Continuous amplification (voltage gain) from unity to 960 was available with the linear amplifier. Amplifier linearity (section III-A) and an acceptable signal-to-noise ratio (45:1 for Cs^{137} photopeak) were verified for gain settings in the range used for all runs. The discriminator unit allowed continuous selection of pulse heights from 0-100 volts (normal calibration units) and differential pulse selection from 0-10 volts. The whole assembly had a resolving time of approximately one microsecond.

D. Count Recording System (Fig. 3)

1. The output of the discriminator, a 20 volt pulse, was transmitted to a decade scaler having better than one

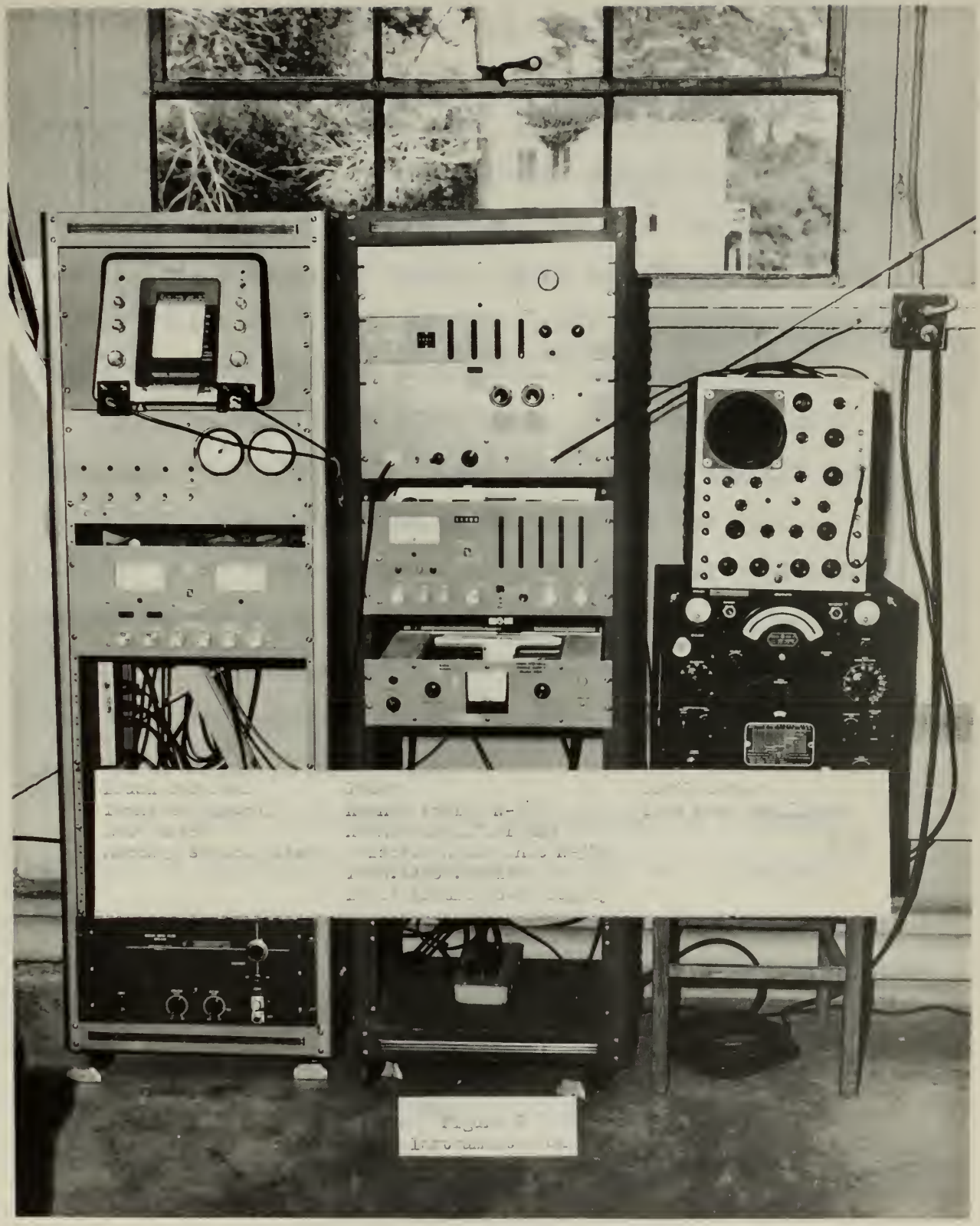

microsecond resolving time. The scaler has been modified by the addition of a 6CB7 cathode follower which acts as an impedance matching device. Thus when the scaler was operating in a continuous mode, scaled output pulses could be fed to the chart recorder without stopping or recycling the scaler. Scaled output pulses could be selected for each 2, 10, 10^2, or 10^3 input pulses to the scaler. The scaled pulses were sent through a differentiating-clipping circuit and then to the continuous chart recorder.

2. The continuous recorder is a two-channel chart type with variable chart speeds of 1, 5, 25, and 125 mm/sec. It is capable of recording up to about 110 cps with a minimum input sensitivity of 10 m.v. For this application, output pulses from the scaler, representing a scaled number of counts, were recorded in one channel and a calibrating time mark was recorded in the other.

E. Time Calibration System

The basic instrument for this system is a crystal controlled oscillator designed primarily as a frequency standard for radio frequency calibration. Frequency standards of 10, 20, or 100 kilocycles, with rated stability of .005%, could be selected. Pulses of desired frequency were transmitted via shielded cable to a five-decade, 200 kilocycle scaler. The scaler was modified to act as a frequency divider by tapping off the third or fourth stages,

thus giving a wide selection of time calibrating pulses (10^{-1}, 1, 10, etc, seconds per pulse interval). The time pulses, after differentiation and clipping, gave a single sharp spike per scaled number of input cycles and an accurate record of time on the recorder chart.

III. Calibration and Procedure

A. Energy Calibration

1. A planchette containing an evaporated Cs^{137} sample was used as a calibrating source. The known γ energy (662 Kev) and long half life (30 yr.) suited it to this use. The planchette was secured in a phenolic holder which was machined to fit over the crystal case (Fig. 4). The holder and crystal case were scribed so that a reproducible position was available.

2. The amplifier linearity was adjusted according to the manufacturer's instructions. An output pulse from a mercury switch pulser that matched the pulse shape of the signal from the preamplifier was used. At the same time, for convenience, the amplifier was calibrated so that the lower discriminator (E) settings gave the approximate pulse height in volts. The use of Cs^{137} for an energy calibration source and knowledge that the primary gamma energies of the nuclides of interest lay under 662 Kev, led to the choice of approximately 90 v. (.9 of full scale) for the position of the Cs^{137} photoline. Gain settings on the amplifier were adjusted so that the photoline fell at roughly 90 v. when observed on a cathode ray oscilliscope. Exact position of the photopeak was determined from a differential energy spectrum and found to be at 98.5 volts as read on the lower level discriminator

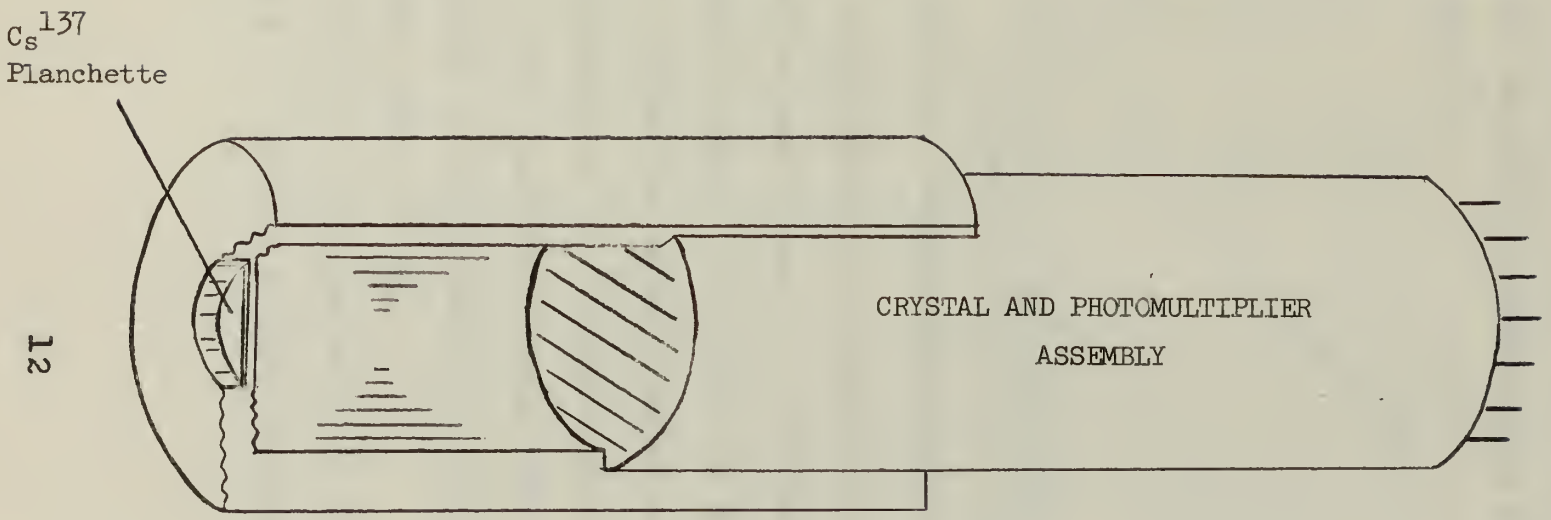

FIGURE 4

Calibration Source and Holder

scale. Thus the discriminator dial setting was calibrated versus gamma energy. A check on the linearity of the entire system and verification of the calibration described above was obtained by measuring the photopeak position of the 364 kev gamma from I^{131}. Results are shown in Fig. 5.

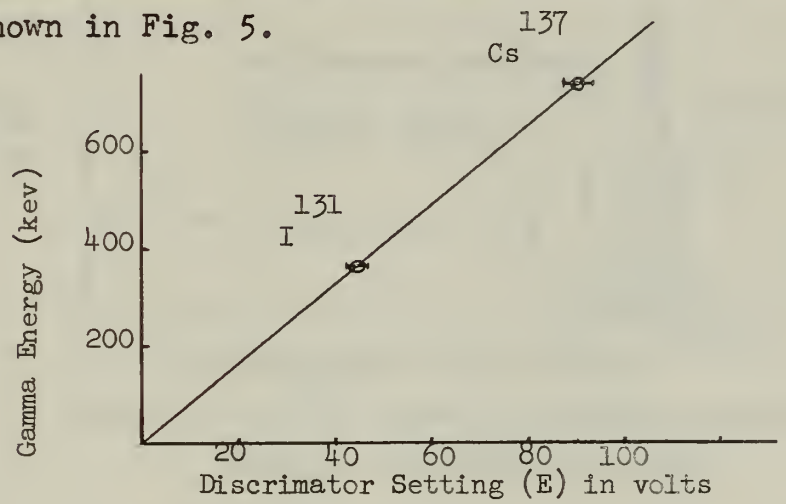

Fig. 5. Energy Calibration Curve

Periodic checks using the mercury switch pulser as the input, and an oscilliscope to determine pulse heights of the amplifier output, indicated no departure from amplifier linearity within the uncertainties of the measurements.

Calibration of the differential discriminator, or "window", gave a maximum window width of 8.3 volts, corresponding to approximately a 60 kev energy interval on the curve shown in Fig. 5.

3. Daily gain adjustments to provide energy calibration were made by a "quick" method suggested by H. E. Handler /8/.

Initially, this method required the selection of a reference discrimination setting and measurement of the corresponding integral rate immediately after obtaining the Cs^{137} spectrum. A value near the midpoint of the

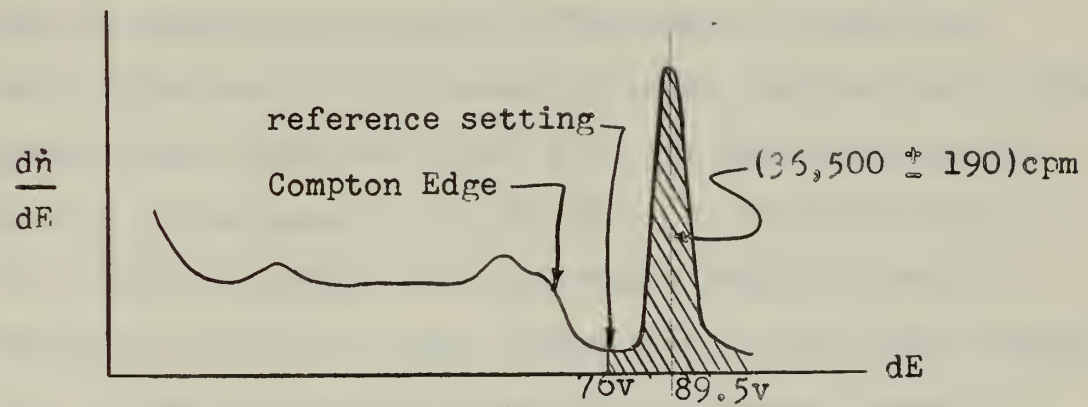

Fig. 6. Cs^{137} Spectrum Showing Reference Voltage and Reference Rate

"valley" between the Compton edge and the photopeak was chosen as the reference discriminator setting. This choice of setting makes the corresponding integral count least susceptible to small gain changes. At this setting, 76 volts on the lower discriminator, the integral rate (corresponding to the area under the curve) was measured as (36,500 ± 190) counts per minute. Once this rate was determined it became a reference for future measurements. Subsequent energy calibrations were made by first adjusting the amplifier gain to give the approximate desired pulse height of the reference photopeak as measured on an oscilliscope. Then fine gain adjustments were made at the

reference discriminator setting to attain the reference counting rate.

B. Gain Stability

The fact that certain photomultiplier (PM) tubes exhibit marked gain shifts (effectively a change in multiplication) at high counting rates, particularly rates greater than 5000 counts per sec, has been reported by several investigators /9, 10, 11/. D. F. Covell and B. A. Euler at NRDL, in an extensive study of various brands and types of tubes, found that of the tubes showing gain shifts, all required an hour to several hours to recover*. R. Chery corroborated this information when he found PM tubes would be very stable for pericds of about 24 hours if they were first exposed for 20-30 hours to high (just below tube dissipation limits) gamma radiation levels.

This slow tube recovery has been utilized to advantage in this experiment by presaturating the PM tube prior to the decay runs. The sample was irradiated at the same power level and for the same irradiation time as for the actual decay run. Reference rates were checked after this exposure and readjusted, as necessary. After decay runs, reference rate checks showed less than 1.5% gain shift (in our case less than .75% reference rate shift), and

*The initial gain shift occurred almost instantaneously.

tube recovery times lasted up to several hours. In all cases, recovery times were very much greater than the maximum counting period used (five minutes). The effectiveness of the technique was substantiated in subsequent analyses of the data (Section IV), which indicated no appreciable systematic errors as would have been the case with large gain shifts.

An alternate method for checking gain shift consisted of placing a Cs^{137} sample near the crystal during measurement runs to give a steady high background rate. This rate (~150 cps) was measured before and after each run, at operating powers. This method confirmed that gain shift was generally less than 1.0%, and data were not used if the gain shift exceeded 1.5%. Two advantages were gained with this check. The first was that the measurements could be taken without disturbing the crystal assembly. Second, this allowed a visual check during the run by superimposing the Cs^{137} pulse over the measured pulses on the oscilloscope. In this manner any large short-term shifts during measurement could be observed, although none were observed.

Other electronic equipment in the counting system, once stabilized by a three to four hour warm-up period, had negligible drift over the periods of time required to make one or several runs.

C. Measurement of Resolving Time

A double pulse generator was used to determine the resolving time of the counting system. Initially, each component (amplifier, discriminator, and scaler) was checked separately to assure specifications were met.

A test signal circuit is provided in the preamplifier system that allowed checking the system resolving time with the double pulse signal. The results of measurements on the entire system gave a value of (1.4 ± .1) micro-seconds for the resolving time.

D. Activation Parameters

Activation times and reactor powers were varied according to the half life measured and the gamma energy investigated. An effort was made in each case to have an initial recorded count rate of 5,000-10,000 counts per second. This limitation was imposed by the use of the 100 counts per mark scaling factor at the beginning of each run. Rates greater than 10,000 counts/sec approached the recorder frequency limit of about 110 cycles/sec.

The Hafnium activities were measured at gamma energies of (330 ± 30*) kev for Hf^{178m} and (215 ± 30) kev for Hf^{179m}. Hf^{178m} also has a very strong (41%) line at 213.4 kev /11/, but the low activation cross-section ratio

*One-half the energy "window", rather than an error estimate.

/5/ of $\sigma_{act(178)}/\sigma_{act(179)} = .054$ for our sample precluded the use of this energy for the measurement of the shorter-lived nuclide. To eliminate possible degradation of the results for the longer half-life due to pulse pile-up*, the shorter-lived nuclide was allowed to decay before measuring the longer.

In general, activation times of approximately one half-life were selected in order to obtain at least 50% of the saturation activity of the nuclide of interest, yet reduce contributions to the counting rate from any long-lived impurities present. This method proved inadequate for the investigation of the Hf^{178m} nuclide. Consequently, a higher reactor power for a shorter irradiation period was chosen to give a ratio of initial relative activities of at least 3:1 for the Hf^{178m} : Hf^{179m} nuclides.

The integral mode of operation was used in the Yb^{177m} measurement. The low cross-section, about 7 barns for Yb^{176}, would have required an excessive amount of reactor power in order to obtain desired counting rates in the differential mode. The integral discriminator (E dial) was set to eliminate all gamma energies below about 95 kev. In this manner, both the 104 and 212 kev gammas were measured at a considerable savings in reactor power.

*In the case in which two half-lives, say $t_{\frac{1}{2}}'$ and $t_{\frac{1}{2}}''$, are represented in the source, the effective pulse introduces three false half-lives into the measured activity: $\frac{t_{\frac{1}{2}}'}{2}$, $\frac{t_{\frac{1}{2}}''}{2}$, and $\left(\frac{1}{t_{\frac{1}{2}}'} + \frac{1}{t_{\frac{1}{2}}''}\right)^{-1}$.

The following table summarizes the activation parameters and the gamma energies for each type run.

Nuclide	Activation Time	Reactor Power	Gamma Energy
Hf^{178m}	2 sec	20 watts	(330 ± 30) kev
Hf^{179m}	20	1	(215 ± 30)
Yb^{177m}	5	10	all above 90

IV. Data

A. Data Reduction

Data tapes consisted of two channels of simultaneously recorded information; one of time, the other of scaled counting marks (Fig. 7). The "counts" channel was broken down into a series of consecutive time intervals, starting with intervals that were short compared to the measured half-life and increasing in length (time) as the counting rate decreased and approached the background level. Short intervals were chosen so that the sample would not decay appreciably over any given counting interval. The approximate expression for the measured rate,

$$R_n \cong \frac{1}{\Delta t} \int_{t-\frac{\Delta t}{2}}^{t+\frac{\Delta t}{2}} \dot{n} \; dt,$$

is valid only for the case of Δt small compared to $t_{\frac{1}{2}}$; where n is the instantaneous counting rate at the midpoint (t) of the n^{th} interval (Δt) and R_n is the measured number of counts per interval Δt. In each of our decay analyses, intervals of less than 1/7 of the (shortest) half-life were used initially. To ensure adequate statistical accuracy for all intervals containing more than 2500 counts, 25 marks at a scaling factor of 100, the number of counts was estimated to the nearest 50 counts. Similarly, the

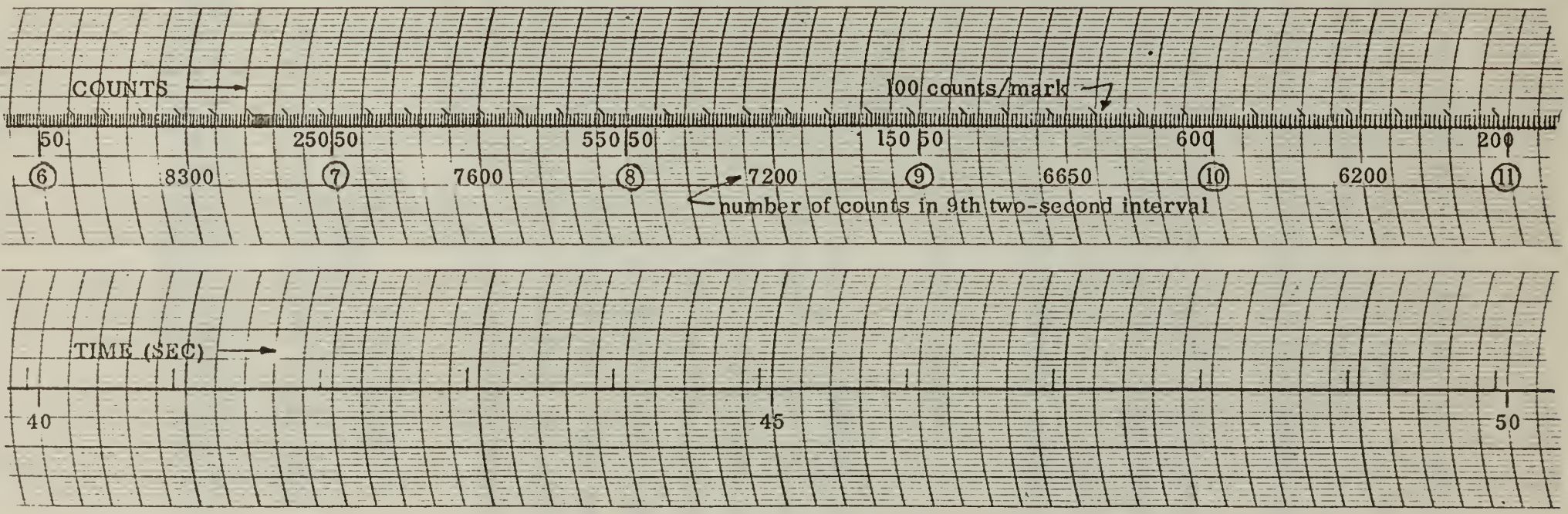

FIGURE 7

Sample Data Tape (section of tape from run shown in sample output, Appendix I)

number, for intervals containing 625-2500 counts, was estimated to the nearest 25 counts. In this manner the counts in each interval were estimated to within the standard deviation calculated according to Poisson statistics.

The timing error was estimated by measuring the drift of the calibrating marks in the "time" channel with respect to the printed grid. Typical of the values obtained in these measurements (taken over the entire counting period) was 1×10^{-3} sec/sec.

B. Analysis (least squares program)

1. Theory

The data for the two component decay of the Hf sample and for the single decay of the Yb sample were analysed with the aid of a CDC 1604 computer. In the iterative least squares analysis program (FRANTIC)* the input data points (R_n) are corrected for dead time (T_d) and background (B). Then each point is normalized (XNORM) as desired (in this case XNORM = 1.00 was used) to yield the correct data (A_n) for the n^{th} data point,

$$(1)\quad A_n = \left[\frac{Rn}{1-R_nT_d} - B\right] \text{XNORM}$$

A statistical weight factor (W_n) is then applied,

*This discussion will necessarily be limited to the main points of the analysis. For further clarification refer to item #6, Bibliography.

which is of the form:

$$(2)\quad W_n = \frac{1}{\sigma^2(\text{total})_n\ (\text{XNORM})^2}$$

where $\sigma^2(\text{total})_n$, the total variance for the n^{th} point, consists of the sum of the variances for 1) count rate uncertainty 2) background uncertainty 3) uncertainty in dead time and 4) uncertainty in the time length of the counting interval.

For finite observation intervals (DT_n), the expression for the activity (AC_n) resulting from N radioactive decays is:

$$(3)\quad AC_n = \sum_{i=1}^{N} A_{o_i}\, e^{-\lambda_i T_n}\, \frac{1 - e^{-\lambda_i DT_n}}{\lambda_i DT_n}$$

This exact expression is not properly evaluated by the computer for small values of $\lambda_i DT_n$ so that equation (3) is expressed in terms of a hyperbolic sine function and expanded to give the expression:

$$(4)\quad AC_n = \sum_{i=1}^{N} A_{o_i}\, e^{-\lambda_i (T_n + DT_n)} \left[1 + \frac{x^2}{3!} + \frac{x^4}{5!} + \frac{x^6}{7!} + \ldots\right]$$

$$\text{where } x = \frac{\lambda_i DT_n}{2}$$

In the least squares fit analysis this expression is used for values of $\lambda_i DT_n$ up to 1.0 and the original expression (3) is used for values of $\lambda_i DT_n$ greater than

1.0. The λ_i values are then held fixed and the above expressions are linear in the A_{0_i} coefficients.

In the iterative least squares analysis the exact expression (3) is expanded in a Taylor series about the point defined by the values of A_{0_i} and λ_i from the preceding iteration.

The iterative process is continued until all parameters, as well as the weighted variance of fit (the square of the standard deviation of the distribution of residuals about zero), deviate from their value in the preceding iteration by not more than one part in 10^6, or until 25 iterations have been completed.

A sample of the computer output from a measurement of Hf^{179m} is included as Appendix I.

2. Goodness of Fit

Of particular interest in this program is the goodness of fit information included in the printout. χ^2, the weighted variance of fit (VAR), and a histogram of the distribution of the residuals (of the experimental curve about the calculated curve) are given. In using the usual χ^2 vs. degrees of freedom tables, the weighted variance of fit (VAR) times the degrees of freedom (DF)* will give a more realistic measure than χ^2 of the probability of

*In this case degrees of freedom is defined as the number of input data points minus the number of parameters allowed to float.

performing a better experiment or finding a better fit with different parameters or a different hypothesis. This is true since the uncertainties in dead time, background, and length of time interval are considered in the calculation of VAR, whereas they are not in calculating χ^2.

As an example, using the output data shown in Appendix I, VAR x DF = 27.558 (with 29 degrees of freedom). This gives a 91.5% "assurance" that the calculated fit is unique for the given data, i.e., that the hypothesis proposed is correct. The histogram of the distribution of the residuals is approximately Gaussian, as it should be. In this case, had a two component decay mode been proposed in the initial estimates, the anlysis would have either rejected the second mode or given a large VAR indicating a false hypothesis.

In general, an arbitrary criterion for rejecting data was established. A significance level (α) of .10 was chosen for the individual runs. This means that we accepted a 10% chance of making an error when rejecting a result as false; or, conversely, only 10% of the time, over a series of many runs, would true results fall outside of our criterion. In the example mentioned above the value of α for this run would be .915, meaning a 91.5% chance of being incorrect if the results were rejected as false. As an example of a run that was rejected; the

VAR x DF was 61.65. From the χ^2 vs. degrees of freedom tables, we find that there is only a 5% chance of being incorrect in rejecting this result /14/.

3. Method of Weighting Results

Results of the half life measurements were weighted according to the "goodness of fit" of the least squares analysis.

The weight factor, c_i, applied to each result is:

$$c_i = \frac{1}{\sigma_i^2}$$

where: $\sigma_i = (\text{VAR} \times \text{AM}^{-1})^{\frac{1}{2}}$

VAR = weighted variance of fit

AM^{-1} = the inverse of the least squares matrix in the analysis.

This σ_i value is the value given as the half life "sigma" (App.I) in the computer program output for the particular run considered.

Using this weight factor the half life, $t_{\frac{1}{2}}$, is found by:

$$t_{\frac{1}{2}} = \frac{\sum_{i=1}^{n} c_i \, t_{\frac{1}{2}i}}{\sum_{i=1}^{n} c_i}$$

where: $t_{\frac{1}{2}i}$ = the half life for the i^{th} run

n = number of runs used.

The standard deviation of the half life, $\sigma(t_{\frac{1}{2}})$, is calculated from:

$$\sigma(t_{\frac{1}{2}}) = \left[\frac{1}{\sum_{i=1}^{n} c_i} \right]^{\frac{1}{2}}$$

V. Results

In the analysis of the data the mode of decay (i.e., two component or one component) used in the program depended on the half life being measured. In the case of Hf^{178m} a two component decay was assumed. For Hf^{179m} and Yb^{177m} single component decays were used. This required, in the case of Hf^{179m}, that the shorter half life be allowed to decay to a small value (less than 1% of total) before measurements were taken.

The tabulated results of the individual acceptable runs for the measurements of the half-lives of the isotopes under consideration are as follows:

Hf^{177} (n, γ) Hf^{178m} (.326 Mev transition measured)

Half-life	Sigma
3.774 sec.	.177 sec.
3.996	.209
3.952	.057
3.917	.060

Hf^{178} (n, γ) Hf^{179m} (.217 Mev transition measured)

Half-life	Sigma
18.485 sec.	.092 sec.
18.519	.073
18.509	.168
18.574	.099
18.373	.090

Yb^{176} (n, γ) Yb^{177m} (.212 Mev transition measured)

Half-life	Sigma
6.564 sec.	.092 sec.
6.470	.046
6.466	.046
6.542	.091

The weighted averages resulting from these measurements are:

Isotope	Half-life
Hf^{178m}	(3.92 ± .05)sec.
Hf^{179m}	(18.49 ± .04)sec.
Yb^{177m}	(6.49 ± .03)sec.

The value of 18.49 sec for the half-life of Hf^{179m} agrees with the value of 18.6 ± .8 reported by Alexander and Brinckmann.

The value of 3.92 sec. for the half-life of Hf^{178m} falls almost exactly between the measurements of 3.5 sec. reported by Campbell and Fettweis, and the 4.3 sec. value reported by Alexander and Brinckmann.

The value of 6.49 sec. for the half-life of Yb^{177m} is in good agreement with the value of 6.5 sec, also reported by Campbell and Fettweis.

Assuming that there are no appreciable systematic errors, it would appear that the present system of recording and analysing decay data is capable of good precision. Thus we are led to prefer the single channel device for the following reasons:

1) The system dead time is considerably less than that encountered with multi-channel analysers (1.4 micro-sec vs. 20-50 micro-sec for many multi-channel devices). Smaller dead time allows working with higher activities, hence better precision in counting data.

2) The dead time factor and overall timing error can be accurately determined for the single channel instrument. Variations which occur in "live" (on) times and switching (off) times between channels make evaluation of actual counting times and dead times a difficult task with multi-channel devices.

It is felt that the present system, with the FRANTIC computer program, can be effectively used to measure half-lives on the order of 0.5 seconds.

BIBLIOGRAPHY

1. E. der Mattsorian and M. Goldhaber, Physical Review, 76:1, 187 (1949).

2. A. Flammersfeld, Naturwiss, 32:36 (1944).

3. E. C. Campbell and P. F. Fettweiss, Nuclear Physics, 33:272-84 (1962).

4. E. C. Campbell and P. F. Fettweiss, Nuclear Physics, 13, 92 (1959).

5. K. F. Alexander and H. F. Brinckmann, Nuclear Physics, 32:3, 482-9 (1962).

6. P. C. Rogers, FRANTIC Program for Analysis of Exponential Growth and Decay Curves, Massachusetts Institute of Technology, TR-76, June 1962.

7. A. O. Paas and R. D. Sullivan, Measurement of Neutron Activated Short-Lived Nuclides Using a Pneumatic Transfer System (Thesis), U. S. Naval Postgraduate School, 1962.

8. H. E. Handler, Gamma-Gamma Angular Correlation in the Decay of Cl^{34}, (Thesis), University of California at Los Angeles, 1955.

9. D. F. Covell and B. A. Euler, Gain Shift Versus Counting Rate in Certain Multiplier Phototubes, U. S. Naval Radiological Defense Laboratory, T.R. 521, 8 June 1961.

10. R. Chery, Journal de Physique et le Radium 21:8-9, 679-680 (1960).

11. R. K. Smither, Physics Division Summary Report, Argonne National Laboratory, ANL-6517, Feb.-Mar. 1962.

12. S. Burson, et. al., Physical Review, 83, 62 (1951).

13. Nuclear Data Sheets, National Academy of Sciences National Research Council, 1959.

14. W. F. Dixon and F. J. Massey Jr., Introduction to Statistical Analysis, McGraw-Hill Book Co., Inc. N.Y.,1957.

15. L. G. Parratt, Probability and Experimental Errors in Science, John Wiley and Sons, Inc., New York, 1961.

ANALYSIS OF HF(179M) 3 MAY 63 RUN NO. 2 1W, 18 SEC

INPUT B	= FRANTIC IDENTIFICATION	32.00000	= TAU (TIME TO COUNTING)
1	= NUMBER OF COMPONENTS	1.40000	= TAUD (DEAD TIME FACTOR IN MICRO TIME UNITS)
0	= NUMBER OF PARAMETERS HELD FIXED	.10000	= ERROR IN DEAD TIME FACTOR (MICRO TIME UNITS)
31	= NUMBER OF DATA POINTS	74.40000	= BACKGROUND
29	= DEGREES OF FREEDOM	.00143	= UNCERTAINTY IN TIMING INTERVAL IN TIME UNITS
8	= ITERATIONS	1.00000	= DATA SCALE FACTOR
2	= STATISTICAL WEIGHTS	1.00000	= NORMALIZATION FACTOR
0	= NUMBER OF POINTS (*) DEVIATING MORE THAN 2 SIGMA		
16582.03153	= LEAST SQUARES DETERMINANT		
.00030	= DELTA VARIANCE OF FIT X 10(6)		
.95027	= WEIGHTED VARIANCE OF FIT		
31.58733	= CHI SQUARE		

A(ZERO)	SIGMA	LAMBDA	SIGMA	N(ORIGINAL)	SIGMA	HALF LIFE	SIGMA
18992.120	156.790	.037428824	.000146553	1680860.	15358.	18.5191	.0725
ORIGINAL ESTIMATES							
18560.890		.037000000					

ANALYSIS OF THE DEVIATIONS

SIGMA	-XS	-4.5	-4.0	-3.5	-3.0	-2.5	-2.0	-1.5	-1.0	-0.5	-0.0	0.0	0.5	1.0	1.5	2.0	2.5	3.0	3.5	4.0	4.5	XS
	0	0	0	0	0	0	0	1	3	6	6	6	3	2	4	0	0	0	0	0	0	0

	BEGINNING TIME	INTERVAL TIME	ORIGINAL COUNTS	CORRECTED DATA	CALCULATED RATE	INSTANTANEOUS RATE	WEIGHTS X 10(3)	DELTA RATE
1	32.000	2.000	11300.0	5620.648	5524.023	5522.734	.34614	96.625
2	34.000	2.000	10250.0	5087.638	5125.606	5124.410	.38165	-37.969
3	36.000	2.000	9500.0	4707.399	4755.925	4754.815	.41170	-48.526
4	38.000	2.000	8950.0	4428.813	4412.906	4411.876	.43686	15.906
5	40.000	2.000	8300.0	4099.852	4094.628	4093.672	.47080	5.224
6	42.000	2.000	7600.0	3745.924	3799.305	3798.418	.51369	-53.381
7	44.000	2.000	7200.0	3543.836	3525.282	3524.460	.54185	18.553
8	46.000	2.000	6650.0	3266.150	3271.023	3270.260	.58596	-4.873
9	48.000	2.000	6200.0	3039.113	3035.103	3034.394	.62773	4.010
10	50.000	2.000	5700.0	2787.017	2816.198	2815.540	.68165	-29.181
11	52.000	2.000	5350.0	2610.656	2613.081	2612.471	.72523	-2.425
12	54.000	2.000	4950.0	2409.206	2424.614	2424.048	.78234	-15.408
13	56.000	2.000	4650.0	2258.193	2249.740	2249.215	.83142	8.453
14	58.000	2.000	4300.0	2082.091	2087.479	2086.992	.89704	-5.388
15	60.000	2.000	4000.0	1931.216	1936.921	1936.468	.96209	-5.705
16	62.000	2.000	3750.0	1805.535	1797.221	1796.802	1.02394	8.314
17	64.000	2.000	3550.0	1705.022	1667.598	1667.208	1.07943	37.424
18	66.000	2.000	3200.0	1529.192	1547.323	1546.962	1.19250	-18.131
19	68.000	2.000	3100.0	1478.971	1435.723	1435.388	1.22928	43.247
20	70.000	2.000	2800.0	1328.349	1332.173	1331.862	1.35457	-3.823
21	72.000	2.000	2700.0	1278.156	1236.090	1235.802	1.40220	42.066
22	74.000	2.000	2400.0	1127.619	1146.938	1146.670	1.56750	-19.319
23	76.000	4.000	4500.0	1052.375	1025.838	1024.880	3.33302	26.537
24	80.000	4.000	3700.0	851.799	883.198	882.374	4.00053	-31.399
25	84.000	4.000	3275.0	745.290	760.392	759.683	4.47672	-15.103
26	88.000	4.000	2975.0	670.125	654.662	654.051	4.88732	15.463
27	92.000	4.000	2500.0	551.147	563.633	563.107	5.71751	-12.486
28	96.000	4.000	2275.0	494.803	485.262	484.809	6.21775	9.541
29	100.000	4.000	1900.0	400.916	417.788	417.398	7.27911	-16.872
30	104.000	4.000	1765.0	367.123	359.696	359.360	7.75568	7.427
31	108.000	4.000	1560.0	315.813	309.681	309.392	8.61181	6.132

APPENDIX I

Sample Computer Output

Appendix II

Isotope Energy Levels and Decay Schemes

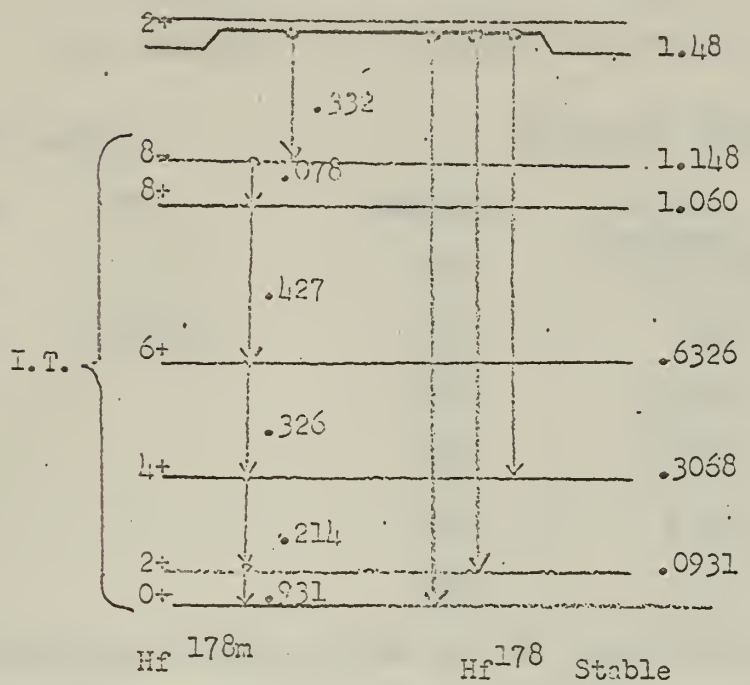

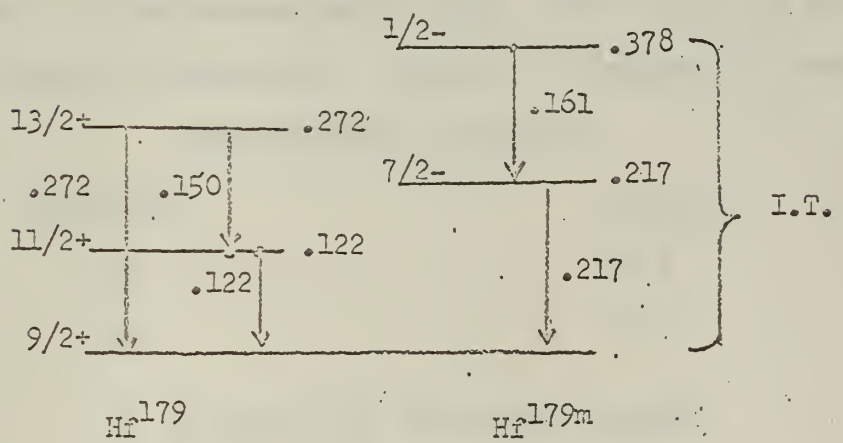

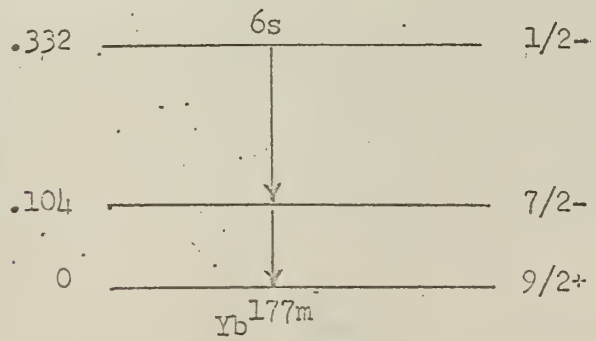

APPENDIX III

Isotopic Analysis of Samples

1. Analysis of Hafnium Sample

(as reported by Oak Ridge Analysis)

Element Hafnium		Isotopic Analysis		
Isotope	177	Isotope	Atomic percent	Precision
Series	G. P.	174	trace only	
Sample	827 (a)	176	.99	± .07
		177	59.08	± .52
		178	31.73	± .49
		197	4.53	± .17
		180	3.68	± .11

The limits quoted above are an expression of the precision of this measurement only. The error is estimated at less than 1% from known sources of systematic errors.

Spectroscopic Analysis

Element	Percent
Cu	0.1
Fe	0.2

2. Analysis of Ytterbium Sample

(as reported by Oak Ridge Analysis)

Element Ytterbium

Isotopic Analysis

Isotope	176	Isotope	Atomic percent	Precision
Series	IU			
Sample	1061 (a)	168	< .01	
		170	< .02	
		171	.11	
		172	.26	± .05
		173	.30	± .05
		174	1.81	± .05
		176	97.57	± .1

The limits quoted above are an expression of the precision of this measurement only. The error is estimated at less than 1% from known sources of systematic errors.

Spectroscopic Analysis

Al < .05	Ni < .05	Gd < .004
Ba < .02	Pb < .1	Tb < .05
Be < .001	Si < .05	Dy < .1
Ca < .07	Sn < .05	Ho < .02
Co < .05	Ti < .02	Fr < .004
Cr < .05	V < .02	Tm < .02
Cu < .05	Zr < .1	Lu < .018
Fe < .02	Y < .004	
K < .01	La < .01	< = No spectrum line visible. Probably absent, definitely less than value given.
Li < .01	Ce < .2	
Mg < .02	Pr < .1	
Mn < .02	Nd < .1	
Mo < .05	Sm < .1	
Na < .05	Eu < .004	